Volume 1 | Number 1 | Jan 2013 | Pages 1–100

Journal of
Materials Chemistry A

Materials for energy and sustainability
www.rsc.org/materialsA

Li+

ROYAL SOCIETY
OF CHEMISTRY

ROYAL SOCIETY
OF CHEMISTRY

www.rsc.org/materialsA

Separated-structured all-organic dielectric elastomer with large actuation strain under ultralow-voltage and high mechanical strength

Ming Tian[1, 2 *], Yang Yao [1], Suting Liu [1, 2], Dan Yang [1, 2], Liqun Zhang[1, 2],

Toshio Nishi[3], and Nanying Ning[1, 2 *]

1. State Key Laboratory of Organic-Inorganic Composites, Beijing University of Chemical

Technology, Beijing 100029, China;

2. Key Laboratory of Carbon Fiber and Functional Polymers, Ministry of Education,

Beijing University of Chemical Technology, Beijing 100029, China;

3. Department of Applied Physics, The University of Tokyo, Hongo, Bunkyo-ku, Tokyo,

Japan.

Abstract: We report the design and preparation of a separated-structured all-organic dielectric elastomer (DE) with large actuation strain under ultralow-voltage and high mechanical strength. Based on the protonic-conductivity mechanism of gelatin, novel organic conductive filler with high dielectric constant and low elastic modulus was prepared by mixing gelatin and glycerol (GG). The separated structured DE was prepared by spraying the solution of GG into the multi-layers of thermoplastic polyurethane elastomer (TPU) nonwoven fabric by electrospinning followed by hot pressing under vacuum. The densely packed TPU nonwoven fabric not only ensure the good mechanical strength of GG/TPU DE, but also separate GG filler and stop the formation of GG continues phase, preventing the

---
[*]**Corresponding author.** Email:tianm@mail.buct.edu.cn (M. Tian), ningny@mail.buct.edu.cn (N. Ning).

formation of conducting path under exerted electric field. The novel GG filler greatly increase the dielectric constant and decrease the elastic modulus of the GG/TPU DE. As a result, the as-prepared DE exhibits good mechanical strength and 5.2% actuation strain at a very low electric field (0.5 kV/mm). To the best of our knowledge, the required electric field for the same actuation strain is the lowest compared to other DE reported in literatures. Since all components in this composite are organic and biocompatible, this study offers a new method to prepare a DE with large actuation strain at low electric field for its application in biological and medical fields, where a low electric field is required.

Keywords: dielectric elastomers, separated-structure, actuation strain, electrospinning, gelatin and glycerin (GG)

1. Introduction

Dielectric elastomer actuators (DEAs) can convert electric energy to mechanical energy without gearing and work efficiently over a broad frequency range, thus have been receiving much attention in the past two decades.[1] DEAs find applications in many fields such as haptic displays,[1] optical lenses,[2, 3] flat-panel speakers, micro-robotics,[4] and artificial muscles[5] because of their large strain, fast response, high energy density, high electromechanical coupling efficiency, reliability, flexible design and lightweight.[6, 7, 8] In addition, their application in electrical power generators is also of high interest.[1]

Although having a number of intrinsic advantages over existing actuator

technologies, some major limitations of DEAs pose great challenges to their broad utilization. A key limitation is the need for high voltages to drive them, which are still above 1 kV under high electric fields (>100 MV/m) for high-strain DEAs.[9, 10, 11] The high voltages are a major safety concern, which could be harmful to human body and damage equipment, particularly in biological and medical fields, e.g. biomedical devices, biomimetic robots and toys.[3][12] In addition, it is of considerable cost and large volume.

A DEA consists of a thin dielectric elastomers (DE) film sandwiched between two compliant electrodes. An electrostatic pressure is exerted on the film by applying an electric voltage across the thickness direction. As a result, a DEA shrinks in the thickness direction and expands in the plane direction.[13] The strain in thickness direction (S_z) is given by:

$$S_z = p/Y = \varepsilon_r \varepsilon_0 E^2 / Y = -\varepsilon_r \varepsilon_0 (U/d)^2 / Y \qquad (1)$$

where p is the electrostatic pressure exerted on the film, Y is the elastic modulus, ε_0 and ε_r are the dielectric constant of free space and the dielectric constant of the polymer, respectively, E is the applied electric field, U is the applied voltage, and d is the thickness of the film.[7]

Based on the law of volume constancy $(1+S_p)(1+S_z)=1$, the planar strain S_p can be approximated by

$$S_p = \frac{1}{1+S_z} - 1 \qquad (2)$$

According to equation (1), the operating voltage can be lowered by reducing the thickness of the DE film, increasing the dielectric constant or decreasing the elastic

modulus.[14]

Up to now, many studies have been focused on reducing operating voltages by increasing the dielectric constant (ε_r) through introducing high-dielectric-constant ceramics such as BaTiO$_3$,[15] or inorganic conductive fillers such as metal particles and carbon nanotubes into the elastomer matrix. However, the introduction of these stiff fillers into elastomer matrix increases the elastic modulus, leading to a loss in flexibility.[16, 17, 18] As a result, the reduction of operating voltages has been far less than expected. Some highly polarizable conjugated conductive polymers with high dielectric constant such as poly (hexylthiophene),[9] polyaniline(PANI),[19] and copper phthalocyanine oligomers (PolyCuPc)[20, 21] have also been used to reduce the operating voltages. A disadvantage is that these conjugated polymers are usually prepared by a very complicated chemical synthesis process, and their modulus is still much higher than those of the elastomers. On the other hand, new structured dielectric elastomer with a high dielectric constant and a low elastic modulus were synthesized by chemical grafting of π-conjugated conducting macromolecules, polar ester groups or allyl cyanide groups onto the elastomer macromolecular chains.[9, 22, 23] A disadvantage is that the increase in ε_r is limited.

Silicones, acrylics and polyurethanes are the three most promising groups of DE. Among these materials, thermoplastic polyurethanes (TPU) have good recyclability, large force output, high mechanical strength and high ε_r, thus have received much attention in recent years. Numerous studies have been focused on the achievement of low elastic modulus of DE to obtain high actuation strain.[24, 25] In our previous study,

we improved the dielectric constant of TPU/ Polyethylene glycol（PEG）DE through

the disruption of hydrogen bonds of TPU and the ionic conductivity of PEG.[26]

Meanwhile, the elastic modulus of TPU were greatly decreased by the addition of

high content of PEG, resulting in the great increase in electromechanical sensitivity

(β), and thus the great increase in actuated strain at low electric field. A disadvantage

is that the achievement of low elastic modulus results in the poor mechanical strength.

Therefore, the development of a new method to prepare DE with both high

mechanical strength and low elastic modulus is still a challenge.

In this study, based on the protonic-conductivity mechanism of gelatin, we first

prepared a novel organic conductive filler with good conductivity $(1.3 \times 10^{-3}$ S. m$^{-1})$,

high dielectric constant (>41000 at 100 Hz), and low elastic modulus (0.5 MPa) for

the first time by mixing gelatin and glycerol (GG) at the mass ratio of 1:1. Meanwhile,

we fabricated the TPU nonwoven fabric by electrospinning, as schematically shown

in Figure 1a. GG/TPU dielectric elastomers with densely packed TPU submicro-fibers

separated GG fillers was then prepared by spraying the solution of GG into the

as-prepared multi-layers of TPU fabrics followed by hot pressing under vacuum, as

schematically shown in Figure 1b. The densely packed TPU nonwoven fabric could

not only ensure the good mechanical strength of GG/TPU dielectric elastomers, but

also separate GG filler and stop the formation of GG continues phase, preventing the

formation of conducting path under exerted electric field. GG filler could greatly

increase the dielectric constant and decrease the elastic modulus, and thus could

greatly increase the actuation strain of the GG/TPU DE at low electric field, as shown

in Figure 1c. Our goal is to prepare an organic and biocompatible DE with large actuation strain at a low electric field and high mechanical strength for its application in biological and medical fields, where a low electric field is required.

2. Experimental Section

2.1 Materials

Thermoplastic polyester-polyurethane (TPU, Elastollan Soft 85A, 1.21 g/cm^3) was purchased from BASF Polyurethane Specialties Co., Ltd (China) and dried at 60 °C for 5 h before use. Gelatin (150L138) was purchased from Rousselot (Netherlands). Glycerin with the molecular weight of 92.09 was supplied by Beijing Chemical Works (China). N, N-dimethylform-amide (DMF, 99.5%), tetrahydrofuran (THF, 99.0%), acetic acid (CH$_3$COOH, 99.5%), and ethyl acetate (C$_4$H$_8$O$_2$, 99.5%) were supplied by Beijing Modern Oriental Fine Chemistry Co., Ltd. (China).

2.2 Preparation of GG filler

To obtain GG filler with both good dielectric properties and low elastic modulus, we first optimized the ratio of gelatin and glycerin. GG films with different ratios of gelatin and glycerin (1:0, 1:0.2, 1:0.5, 1:1) were prepared by solution casting. Gelatin was dissolved in a mixed solvent (acetic acid: ethyl acetate: deionized water = 6:3:1 by volume ratio) at a concentration of 15 wt% and different amount of glycerin was then added into the solution by stirring. Finally, the GG films were obtained by drying under vacuum for 72 h at 28 °C.

2.3 Preparation of GG/TPU dielectric elastomers

A schematic representation of the preparation of GG/TPU dielectric elastomers is shown in Figure 1. TPU was dissolved in mixed solvent (THF: DMF=7:3 by volume ratio) at a concentration of 10 wt% for electrospinning. TPU submicro-fibers were prepared by electrospinning under room temperature with an injection rate of 1 ml/h, and the applied voltage of 12 kV (ES30P, Gamma High Voltage Research Inc., USA). Electrospinning is a reliable method to produce non-woven mat. By control the condition of electrospinning, i.e. temperature, humidity, the viscosity of electrospinning solution, injection rate, and speed of receiver, we can obtain TPU non-woven mats with stable mechanical properties and porosity. TPU nonwoven fabrics with the thickness of 0.2 mm was then obtained by densely packing multi-layers of the as-prepared submicro-fibers. The porosity of the TPU mat is approximately 33.43%, which are obtained by calculating the volume ratio of GG filler and GG/TPU composite. Meanwhile, gelatin was dissolved in a mixed solvent (acetic acid: ethyl acetate: deionized water = 6:3:1 by volume ratio) at a concentration of 15 wt% and the same content of glycerin was then added into the solution by stirring. The obtained solution of gelatin and glycerin was named as GG solution. The viscosity of the GG solution is 110 cp, which was measured by DV-III Ultra Rheometer (Brookfield, USA) at 25 °C under speed of 20 r/min and torque of 36.7 Nm. GG solution was then sprayed into TPU fiber film by using an air brush to enable GG filler to fully occupy the available inner space between TPU fibers. The samples were then hot pressed and dried under vacuum at 28 °C for 72 h to completely remove the solvent. Finally, GG/TPU composite film with a thickness of 0.2 mm was prepared by hot-pressing at 110 °C under vacuum for 10 min. The mass ratio of GG: TPU are 0.25:1 and 0.5:1 in the as-prepared composites.

2.4 Characterization

The change of hydrogen bonds of gelatin by adding glycerin was characterized by a

Fourier transform infrared (FTIR) spectrometer (Tensor 27, Bruker Optics GmbH, Germany) with the attenuated total reflection (ATR) technique. The angle of incidence was set at 45° by using a ZnSe crystal. The operating conditions were 4 cm^{-1} resolution with 32 scans.

The dielectric properties of GG filler and the GG/TPU composites in the frequency range of 10^2 to 10^6 Hz at 25 °C, 35 °C, 37 °C, and 40 °C were measured by a Broadband Dielectric Spectroscopy (Alpha-A, Novochtrol, Germany). The samples had a diameter of 25 mm and a thickness of 0.5 mm. The mechanical properties of GG filler and the GG/TPU composite were carried out on a tensile apparatus (Instron 11185, Instron Corporation, American) at 25 °C with a stretching speed at 20 mm/min. All samples were cut into the dumbbell shape (20 mm×4 mm×0.2 mm). Elastic modulus (Y) was calculated from slope of stress-strain curve at the strain of 5%, which were obtained by using a tensile apparatus at a strain rate of 2 mm/min.

The morphology of GG/TPU composite was obtained by a S-4800 SEM at 5 kV. For the observation of surface morphology, the samples were first polished and then coated with platinum before SEM observations. For the observation of cross-section morphology, the samples were first cryogenically fractured in liquid nitrogen (-170 °C) and then coated with platinum before SEM observations. For the observation of densely packed separated network structure of GG/TPU composite, the composite was etched by using deionized water for 4 h to remove GG.

The glass transition temperature (T_g) of GG/TPU composites were studied by Differential Scanning Calorimetry (DSC) (STARe, METTLER-TOLEDO,

Switzerland) under N_2 gas atmosphere. All samples were first heated to 100 °C, and held at this temperature for 10 min to erase the thermal history; then cooled to -100 °C with a cooling rate of 10 °C/min. The samples were heated again from -100 °C to 100 °C. The mass of samples tested was 5 ± 0.2 mg.

The conductivity of GG/TPU composites was measured at high resistivity meter (EST 121, Beijing Huajinghui Co., Ltd. China). ρ_v is calculated as follows: $\rho_v = 4\,L/(R_V \times \pi \times d^2)$, where L is the thickness of the specimen, R_V is the volume resistance, and d is the diameter of the electrode.

A circular strain test was carried out to measure the actuation strain without prestrain. The compliant electrodes were fabricated by spraying graphite suspension composed of graphite, silicone oil and curing agent, on the two main surfaces of the film using an airbrush. The dielectric elastomer film was fixed on a circle frame. The strain was defined as the change in the pixel of the electrodes' area divided by the original pixel. The voltage was supplied by a high-voltage direct current generator (DTZH-60, Wuhan Dotek Electric Co., Ltd., China). In order to obtain the change in the pixel of the electrodes' area, a video camera was fixed above the film to capture the actuator plane before and after applying the voltage with the same focal length, and then the captured video pictures were processed with Photoshop software. The planar strain is calculated according to

$$S_p = (A - A_0)/A_0 \times 100\% \qquad (3)$$

where A is the actuated planar area and A_0 is the original planar area.

3. Results and Discussion

3.1 Gelatin/glycerol (GG) dielectric filler with high dielectric constant and low elastic modulus

Gelatin, the hydrolyzed product of collagen, is a kind of biomacromolecules. Gelatin has a large number of polar functional groups, which are beneficial to the polarization under electric field. However, a large number of $C=O\cdots H-N$ hydrogen bonds exist in gelatin, limiting the mobility of these polarized groups. Glycerin with a large number of hydroxyl groups can disrupt the hydrogen bonds between gelatin molecules, facilitating the mobility of these polarized groups in gelatin. Meanwhile, glycerin can act as a plasticizer to reduce the elastic modulus of gelatin.

Infrared spectroscopy was used to study the change in hydrogen bonds between gelatin molecules with the addition of glycerin. The stretching region of N, N-disubstituted amides in gelatin molecules is located between 1670 cm^{-1} and 1630 cm^{-1}. As shown in Figure 2, the peak of N, N- disubstituted amides shifts from 1659 cm^{-1} for pure gelatin to a lower wave number with the increase in content of glycerin, and it shift to 1652 cm^{-1} for GG at the mass ratio of 1:1. The shift of N, N- disubstituted amides to a lower wave number suggests an increasing average strength of the hydrogen bond because of the disruption of $C=O\cdots H-N$ hydrogen bonds in gelatin, and the formation of new stronger $C=O\cdots H-O$ hydrogen bonds between gelatin and glycerin.

Figure S-1 shows the dielectric properties of GG filler with different mass ratio of

gelatin to glycerin as a function of frequency at room temperature. As shown in

Figure S-1 (a), the dielectric constant at the same frequency of gelatin increases with

the increase in content of glycerin. For example, the ε_r at 100 Hz largely increases

from 14.2 for pure gelatin to 41000 for GG filler with the mass ratio of 1:1. The ε_r at

100 Hz of GG filler is much higher than that of PolyCuPc (ε_r <1000 at 100 Hz).[27]

The greatly increased ε_r of GG is mainly ascribed to the protonic-conductivity of

gelatin plasticized with glycerol.[28] The disruption of hydrogen bonds between the

gelatin molecules by glycerol increases the chain mobility and accelerates the

protonation process of the gelatin. The high mobility of the protons formed during the

protonation of the glycine-proline-hydroxyproline of gelatin under electric fields

results in a high dielectric response, and thus the great increase in dielectric constant.

The ε_r of GG fillers obviously decreases with the increase in frequency. The strong

frequency dependence of ε_r of GG filler is due to the space charge polarization

(delocalized protons) of GG filler.[29] The dielectric loss of GG filler with different

ratio of gelatin and glycerin as a function of frequency at room temperature is shown

in Figure S-1 (b). The dielectric loss of gelatin increases with the increase in the

content of glycerin because of the increase in proton conductivity by adding glycerin.

The tensile strength of GG filler with different mass ratio of gelatin to glycerin is

shown in Figure S-2. The elastic modulus decreases from 12 MPa for GG filler with

the mass ratio of 1: 0.2 to 0.5 MPa for GG filler with the mass ratio of 1:1 because of

the increased plasticizing effect of glycerin on gelatin. According to the dielectric and

mechanical properties of GG fillers, GG filler with the mass ratio of 1: 1 is used as the

organic dielectric filler for the preparation of GG/TPU dielectric elastomers with both

high dielectric constant and low elastic modulus.

3.2 Microstructure of GG/TPU Composite

The morphologies of the electrospun TPU nonwoven fabric, the as-prepared

GG/TPU composite films, and the films after etching of GG were observed by

scanning electron microscopy (SEM), and the results are shown in Figure 3. As shown

in Figure 3 (a), a large number of macropores with the size less than 5 microns were

formed in the TPU nonwoven fabric, facilitating the filling of GG filler. Meanwhile,

the mixed solution of gelatin and glycerol (GG) with the mass ratio of 1:1 was

prepared to obtain both good proton conductivity of GG and low elastic modulus (see

section 3.1). Then, the GG solution was sprayed into the as-prepared TPU nonwoven

fabric, and the mass ratio of GG to TPU were 0.25:1 and 0.5:1 to stop the formation

of GG continues phase on the surface of the film, and ensure that GG was separated

by TPU nonwoven fabric network. Most of the GG solution flowed into the

macropores of TPU nonwoven fabric during spraying, and then formed GG filler in

the macropores after the evaporation of solvents, whereas some GG solution was

remained on TPU submicro-fibers and formed discontinuous GG film on the TPU

submicro-fibers. GG/TPU composite films were then obtained by hot-pressing under

vacuum at the temperature slightly higher than the softening temperature of TPU to

avoid the introduction of air bubble, as shown in Figure 3 (b), (c), (d) and (e).

The surface morphologies of the GG/TPU composite films are shown in Figure 3 (b)

and 3 (d). As the mass ratio of GG to TPU was 0.25:1, most of the macropores were filled with GG filler, whereas some macropores were still unfilled，as shown in Figure 3 (b). As the mass ratio of GG to TPU increases to 0.5:1, almost all the macropores were filled with GG filler，as shown in Figure 3 (d). For both composites films, the densely packed TPU fibers can effectively separate GG filler and stop the formation of GG continues phase. The cross-section morphologies of the GG/TPU composite films are shown in Figure 3 (c) and 3 (e). As the mass ratio of GG to TPU was 0.25:1, a large number of fiber-ends and some macropores were observed. As the mass ratio of GG to TPU increases to 0.5:1, a large number of fiber-ends were observed, whereas macropores were not observed. These cross-section morphologies again indicate that the densely packed TPU fibers can effectively separate GG filler, and stop the formation of GG continues phase. In addition, we can observe a good interfacial adhesion between GG and TPU from both the surface morphology and cross-section morphology of the GG/TPU composites.

The surface and cross-section morphologies of the GG/TPU composite films after etching GG phase are shown in Figure 3 (f) and 3 (g), respectively. Obviously, hot pressing of multi-layers of TPU nonwoven fabric ensures the partial fusion of TPU submicro-fibers, and the heat sealing of these fibers, resulting in the formation of GG/TPU composite with GG fillers separated by the densely packed TPU fibers. These densely packed TPU fibers prevent the connection of macropores with adjacent pores, and thus separate GG fillers and suppress the leakage current.

The separation of GG fillers by TPU submicro-fibers is also evidenced by the

largely decreased conductivity from 1.3×10^{-3} S. m^{-1} for GG filler to 2.3×10^{-7} S. m^{-1} and 5.8×10^{-6} S. m^{-1} for the composites with the mass ratio of 0.25:1 and 0.5:1, respectively, as shown in Table 1. The conductivity of GG/TPU composite is slightly increased with the increase in the mass ratio of GG to TPU from 0.25:1 to 0.5:1, again demonstrating that the 3D closely packed TPU submicro-fibers can separate GG fillers, and thus suppress the leakage current.

On the other hand, the effect of GG on the glass transition temperature (T_g) of the GG/TPU composites were studied by DSC, and the results are shown in Figure S-3. As expected, T_g decreases from -28.0 °C for pure TPU to -36.3 °C and -38.2 °C for the composites with the mass ratio of 0.25:1 and 0.5:1, respectively, demonstrating the good interaction between GG and TPU, ascribed to the similar chemical bonds (amide bond) of gelatin and TPU. Meanwhile, the decrease in T_g of TPU by adding GG also indicates that GG act as a plasticizer for TPU, weakening the interaction between TPU chains at the interface between GG filler and TPU fibers, and thus can decrease the elastic modulus of TPU (see below).

3.3 Mechanical Properties of GG/TPU Composites

Figure 4 shows the stress-strain curves of TPU, GG filler and GG/TPU composite films. As expected, TPU shows a high tensile strength (29.2 MPa), while GG shows a low tensile strength (1.4 MPa). The tensile strength of the GG/TPU composites decreases with the increase in content of GG filler. However, the tensile strength of the GG/TPU composite with the mass ratio of 0.5:1 is still up to 9.7 MPa,

demonstrating that the densely packed TPU nonwoven fabric ensure the good mechanical strength of the composites, facilitating the practical application of DE. In addition, a high elongation at break (>500%) is obtained for all the samples.

The elastic modulus of GG filler and GG/TPU composite films are listed in Table 1. As expected, the elastic modulus of GG/TPU composites decreases with the increase in the content of GG filler. For example, the elastic modulus decreases from 8.7 MPa for pure TPU to 2.8 MPa for the GG/TPU composite with the mass ratio of 0.5:1, facilitating the preparation of DE with large actuation strain at low operation voltage. The decrease in elastic modulus of TPU by adding GG is ascribed to the plasticizing effect of GG on TPU at the interface between GG filler and TPU fibers, as demonstrated by the decrease in T_g (as shown in section 3.2).

The cyclic stress-strain curves of pure TPU and the GG/TPU composites and the corresponding hysteresis loss at 5% of strain are shown in Figure 5. From Figure 5 (a), we can observe that both the stress at certain strain and the elastic modulus decrease with the increase in the content of GG. From Figure 5 (b), we can observe that the hysteresis loss decreases from 9.8% for pure TPU to 7.4% for the GG/TPU composite with the mass ratio of 0.25:1. This could be ascribed to the decrease in energy loss in TPU phase caused by the plasticizing effect of GG on TPU, as demonstrated by DSC results. The hysteresis loss increases to 15.7% for the GG/TPU composite with the mass ratio of 0.5:1. In this case, the decrease in energy loss in TPU phase caused by the plasticizing effect of GG on TPU is almost the same as that of the composite with the mass ratio of 0.25:1 because of the similar T_g of both composites (see Figure S-3).

However, the increased energy loss of GG phase caused by the increased internal friction of GG dominate, leading to the increase in the hysteresis loss of GG/TPU composite with the further increase in content of GG.

3.4 Electromechanical Properties of GG/TPU Composites

Despite of the high protonic-conductivity of gelatin (1.3×10^{-3} S. m^{-1}), all the GG/TPU composites show relatively low conductivity ($<10^{-6}$ S. m^{-1}) because of the separation of GG filler by TPU nonwoven fabric, indicating a typical dielectrics (as shown in Table 1). Figure 6 shows the dielectric properties of pure TPU and GG/TPU composites as a function of frequency at room temperature. The high ε_r of GG leads to a significant increase in ε_r of the GG/TPU composite at the same frequency, as shown in Figure 6 (a). For example, the ε_r of the GG/TPU composite with the mass ratio of 0.5:1 at 100 Hz and 1000 Hz is 629 and 77, respectively, which is much higher than that of pure TPU (6.2). The good interfacial adhesion between GG and TPU caused by their similar chemical bonds (amide bond), as well as large interfacial area between TPU submicro-fibers and microsized GG filler, results in the strong interfacial polarization ability of TPU and thus the high ε_r of the as-prepared composite.

The ε_r of the GG/TPU composites obviously decreases with the increase in frequency. The strong frequency dependence of ε_r of GG/TPU composites is ascribed to the space charge polarization (delocalized protons) of GG filler and interfacial polarization of the composites.[29] We note that using the delocalized charge

phenomenon in a composite is analogous to that in ceramic capacitor. [30]

The dielectric loss of pure TPU and GG/TPU composites as a function of frequency at room temperature is shown in Figure 6 (b). The relaxation peak of dielectric loss of the GG filler occurs at high frequency (10^4 Hz) (as shown in Figure 2 (b)). The relaxation peak shifts to low frequency (10^2 Hz) for the composite with the mass ratio of 0.5:1, and it shifts to lower frequency with the decrease in content of GG filler. The relaxation peak occurs at much lower frequency with the decrease in the content of GG is ascribed that the dipole polarization ability of the functional groups of GG is much easier than that of TPU. The dielectric loss of TPU obviously increases with the increase in the content of GG, ascribed to the increase in DC conductance of the composites caused by the increase in conductivity by adding GG filler.

In addition, we studied the dielectric properties of GG/TPU composites at approximately the temperature of the human body (35 °C, 37 °C, and 40 °C) for the biomedical application of our GG/TPU dielectric elastomers. As an example, the dielectric properties of GG/TPU composite with the mass ratio of 0.5:1 are shown in Figure S-4. The ε_r of the GG/TPU composites obviously decreases with the increase in frequency at a certain temperature, consistent with that obtained at room temperature. The ε_r at the same frequency increases with the increase in temperature because of the increase in proton conductivity of GG and the increase in polarizability of TPU at higher temperature, facilitating the biomedical application of GG/TPU dielectric elastomers. A disadvantage is that the dielectric loss also increases with the increase in temperature.

Clearly, the filling of GG in the macropores of TPU nonwoven fabric network results in the simultaneous increase in ε_r and decrease in elastic modulus of TPU. This is ascribed to the very high ε_r and very low elastic modulus of GG filler. As a result, the electromechanical sensitivity (β) of TPU is greatly increased with the increase in the content of GG filler, as shown in Table 1. As an example, β largely increases from 0.7 for TPU to 224.7 for the GG/TPU composite with mass ratio of 0.5:1. The large increase in β facilitates the improvement in actuation strain of GG/TPU composites at low electric field.

Figure 7 shows the actuation strain of GG/TPU composite films as a function of electric field. As expected, the actuation strain at the same electric field significantly increases with increasing the content of GG, owing to the increase in β. The largest actuation strain was obtained for the composite with mass ratio of 0.5:1 under the same electric fields. The maximum actuation strain reaches 5.2% at very low electric field (0.5 kV/mm), a 10-fold increase over that of pure TPU (0.5%).

The physical and electromechanical properties of various advanced DE systems reported in previous studies and the GG/TPU composites are listed in Table 2.[9,12,22,23,25] Upon comparison, although the GG/TPU composite in this study has a higher elastic modulus and dielectric loss, it shows a much higher ε_r and β value, thus a much lower electric field (only 0.5 kV/mm) is needed to achieve the planar actuation strain of 5.2% than that of other DEs reported in the literatures. The large actuation strain at a low electric field (0.5 kV/mm) is beneficial for DE to be used in biological and medical fields. On the other hand, the GG/TPU composite shows the

highest tensile strength.

The history dependence of the electromechanical response, as a very important property of DEAs, was also studied. As an example, the actuation strain of the composite with the mass ratio of 0.5:1 was measured for 10 cycles as previously reported in other study,[31] and the results are shown in Figure 8. The applied electric field 0.3 kV/mm, which is lower than the breakdown strength, was applied periodically. Each application period of 10 seconds was followed by an off-interval of 3 seconds. We can observe that the actuation strain is relatively stable with time, a desirable feature of GG/TPU composite in DEA applications.

4. Conclusion

We have developed a novel separated-structured all-organic dielectric elastomer with large actuation strain under ultralow-voltage and high mechanical strength. Based on the protonic-conductivity mechanism of gelatin and glycerin, novel organic conductive filler (GG) with good conductivity, high dielectric constant, and low elastic modulus was prepared for the first time by mixing gelatin and glycerol. A separated-structured dielectric elastomer was constructed by spraying the solution of GG into the electrospun TPU nonwoven fabric with many macropores followed by hot pressing under vacuum. The densely packed TPU nonwoven fabric mat ensures the good mechanical strength of the GG/TPU composites even containing a high content of GG filler. The separation of GG filler by TPU nonwoven fabric mat suppresses the leakage current. As a result, the as-prepared separated-structured

GG/TPU dielectric elastomer exhibits 5.2% of actuation strain at a very low electric field (0.5 kV/mm) as well as a high tensile strength of 9.7 MPa.

Acknowledgements

References:

[1]   F. Carpi, S. Bauer, D. D. Rossi, *Science*. **2010**, *330*, 1759.

[2]   M. Aschwanden, A. Stemmer, *Opt. Lett.* **2006**, *31*, 2610.

[3]   F. Carpi, G. Frediani, S. Turco, D. D. Rossi, *Adv. Funct. Mater.* **2011**, *21*, 4152.

[4]   J. D. Madden, *Science*. **2007**, *318*, 1094.

[5]   P. Brochu, Q.B. Pei, *Macromol. Rapid Comm.* **2010**, *31*, 10.

[6]   R. Pelrine, R. Kornbluh, Q. B. Pei, J. Joseph, *Science*. **2000**, *287*, 836.

[7]   H. Stoyanov, M. Kollosche, S. Risse, D. N. McCarthy, G. Kofod, *Soft Matter*. **2011**, *7*, 194.

[8]   J. S. Huang, D. R. Clarke, S. Shian, Z. Q. Suo, *Adv. Funct. Mater*. **2013**, *23*, 5056.

[9]   F. Carpi, G. Gallone, F. Galantini, D. D. Rossi, *Adv. Funct. Mater*. **2008**, *18*, 235.

[10]   C. Huang, Q.M. Zhang, *Adv. Funct. Mater*. **2004**, *14*, 501.

[11]   L. Z. Chen, C. H. Liu, C. H. Hu, S. S. Fan, *Appl. Phys. Lett.* **2008**, *92*, 263104.

[12]   F. Carpi , D. De Rossi, R. Kornbluh, R. Perline ,P. Sommer-Larsen, in *Dielectric Elastomers as Electromechanical Transducers*, Elsevier, Amsterdam, **2008**.

[13]   D. M. Opris, M. Molberg, C. Walder, Y. S. Ko, B. Fischer, F. A. Nüesch, *Adv. Funct. Mater.* **2011**, *21*, 3531.

[14]   A. OHalloran, F. OMalley, *J. Appl. Phys.* **2008**, *104*, 071101.

[15]   G. Gallone, F. Carpi, D. D. Rossi, G. Levita, A. Marchetti, *Mater.Sci. Eng.* **2007**, *27*, 110.

[16]   D. N. McCarthya, H. Stoyanova, D. Rychkova, H. Raguscha, M. Melzera, G. Kofoda, *Compos Sci Technol.* **2012**, *72*, 731.

[17]   K. Wongtimnoia, B. Guiffardb, A. B. D. Moortèlea, L. Seveyratb, C. Gauthiera, J. Y. Cavailléa, *Compos Sci Technol.* **2011**, *71*, 885.

[18]   S. Rosset, M. Niklaus, P. Dubois, H. R. Shea, *Adv. Funct. Mater.* **2009**, *19*, 470.

[19]   C. Huang, Q. M. Zhang, *Adv. Mater.* **2005**, *17*, 1153.

[20]   M. Molberg, D. Crespy, P. Rupper, F. Nüesch, J. E. Månson, C. Löwe, D. M. Opris, *Adv. Funct. Mater.* **2010**, *20*, 3280.

[21]   C. Huang, Q. M. Zhang, J. Y. Li, M. Rabeony, *Appl. Phys. Lett.* **2005**, *87*, 182901.

[22]   S. Risse, B. Kussmaul, H. Krüger, G. Kofod, *Adv. Funct. Mater.* **2012**, *22*, 3958.

[23]   B. Kussmaul, S. Risse, G. Kofod, R. Wache, M. Wegener, D. N. McCarthy, H. Kruger, R. Gerhard, *Adv. Funct. Mater*. **2011**, *21*, 4589.

[24]   B. Kim, Y. D. Park, K. Min, J. H. Lee, S. S. Hwang, S. M. Hong, *Adv. Funct. Mater*. **2011**, *21*, 3242.

[25]   D. Yang, M. Tian, H. L. Kang, Y. C. Dong, H. L. Liu, Y. C. Yu, L. Q. Zhang, *Materials Letters* **2012**, *76*, 229.

[26]   M. Tian, B. Y. Yan, Y. Yao, L. Q. Zhang, T. Nishi, N. Y. Ning, *J. Mater. Chem. C*, **2014**, *2*, 8388

[27]   H.S. Nalwa, L. R. Dalton, P. Vasudevan*, Eur. Polym. J.* **1985**, *21*, 943.

[28]   A. Al-Kahlout, D. Vieira, C. O. Avellaneda, E. R. Leite, M. A. Aegerter, A. Pawlicka*, Ionics* **2009**, *16*, 13.

[29]   T. Hanai, *Colloid and Polymer Science* **1960**, *171*, 23.

[30]   H.M. AlAllak, J. llingsworth, A. W. Brinkman, G. J. Russell, J. Woods, *J. Appl. Phys*,**1988**, *64*, 6477

[31]   D. Yang, L. Q. Zhang, N. Y. Ning, D. D. Li, Z. Wang, T. Nishi, K. Ito, M. Tian, *RSC Adv*, **2013**, *3*, 21896

Tables

Table 1. Elastic modulus and electromechanical sensitivity of pure TPU and GG/TPU composites

Samples [GG/TPU]	Conductivity [S.m^{-1}]	Elastic modulus [MPa]	Dielectric constant at 100Hz	Loss tangent at 100Hz	Electro mechanical sensitivity, β [MPa^{-1}]	Breakdown strength [kV/mm]	Maximum strain (%)
0:1	1.9×10^{-10}	8.7 ± 0.2	6.2	0.7	0.7	9.8	0.67%
0.25:1	2.3×10^{-7}	4.9 ± 0.1	80.0	2.4	16.3	1.1	3.19%
0.5:1	5.8×10^{-6}	2.8 ± 0.09	629.1	8.7	224.7	0.55	5.21%
1:0	1.3×10^{-3}	0.5 ± 0.04	41226.4	2.4	-	-	

Table 2. Comparison of physical and electromechanical properties for various advanced dielectric elastomers reported in the literatures

Samples	Dielectric constant at 100Hz	Loss tangent at 100Hz	Elastic modulus [MPa]	Electromechanical sensitivity at 100Hz [MPa^{-1}]	Tensile strength [MPa]	Required electric field [kV/mm] at 5.2% planar actuation strain[1]
GG/TPU composite [2]	629.1	8.7	2.8 ± 0.09	223.1	9.7	0.5
PANI/PolyCuPc/PU[19]	136	0.34	-	-	-	13
Silicone-Poly(hexylthio phene) Blends[9]	4.8	0.7	0.03	160.0	0.092	7.4
Organic dipoles grafted silicon[23]	6.5	0.09	5.5	1.2	-	15.5 [3]
Allyl-cyano filled silicone[22]	6.5	0.1	0.3	21.7	-	18
New polyester elastomer[25]	6.2	-	0.1	62.0	0.89	12

1) 5.2% planar actuation strain is equal to -4.94% actuation strain in thickness direction according to equation: $(S_p+1)(S_Z+1)=1$ in which S_p is planar actuation strain and S_Z is actuation strain in thickness direction;

2) The mass ratio of GG to TPU in GG/TPU composites is 0.5:1;

3) The required electric field mentioned in table is the one for reaching 1.5% maximum actuation strain.

Figure captions

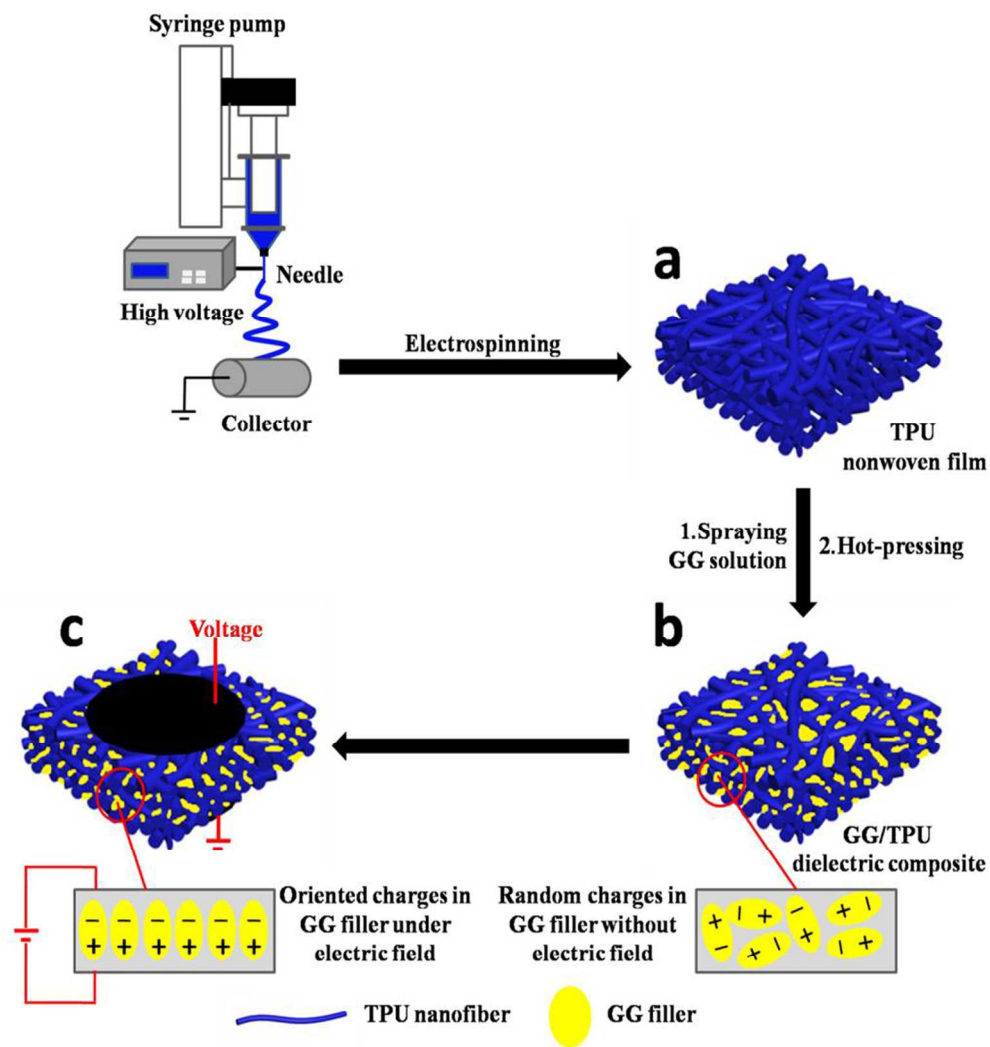Figure 1. Schematic representation of the processing method and the actuation mechanism of GG/TPU dielectric composites

Figure 2. FTIR spectra of GG filler with different mass ratios of gelatin to glycerin

Figure 3. (a)SEM image of electrospun TPU fibers; SEM images of (b) surface morphology and (c) cross-section morphology of the GG/TPU composite at the mass ratio of 0.25:1; SEM images of (d) surface morphology and (e) cross-section morphology GG/TPU composite at the mass ratio of 0.5:1; SEM images of (f) surface morphology and (g) cross-section morphology the GG/TPU composite films at the mass ratio of 0.5:1 after GG phase was etched

Figure 4. Stress-strain curves of pure TPU, GG/TPU composites, and GG filler

Figure 5. (a)The cyclic stress-strain curves of pure TPU and GG/TPU composites and (b) the corresponding hysteresis loss at 5% of strain

Figure 6. (a) Dielectric constant and (b) dielectric loss of pure TPU and GG/TPU composites in the frequency range of 10^2 to 10^6 Hz at room temperature

Figure 7. The actuation strain of TPU and GG/TPU composites at different electric fields

Figure 8. Plot of actuated strain of sample of GG: TPU=0.5:1 against cyclic electric field loading

Figure 1. Schematic representation of the processing method and the actuation mechanism of GG/TPU dielectric composites
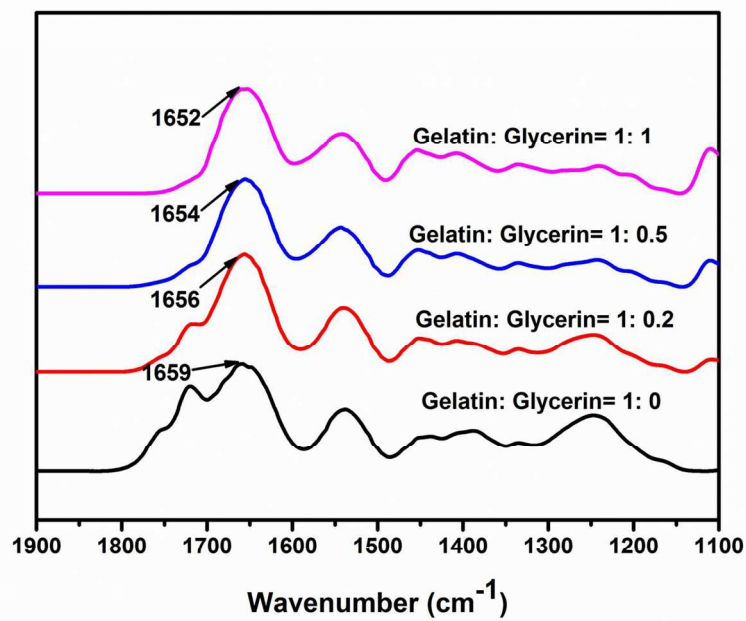174x185mm (150 x 150 DPI)

Figure 2. FTIR spectra of GG filler with different mass ratios of gelatin to glycerin
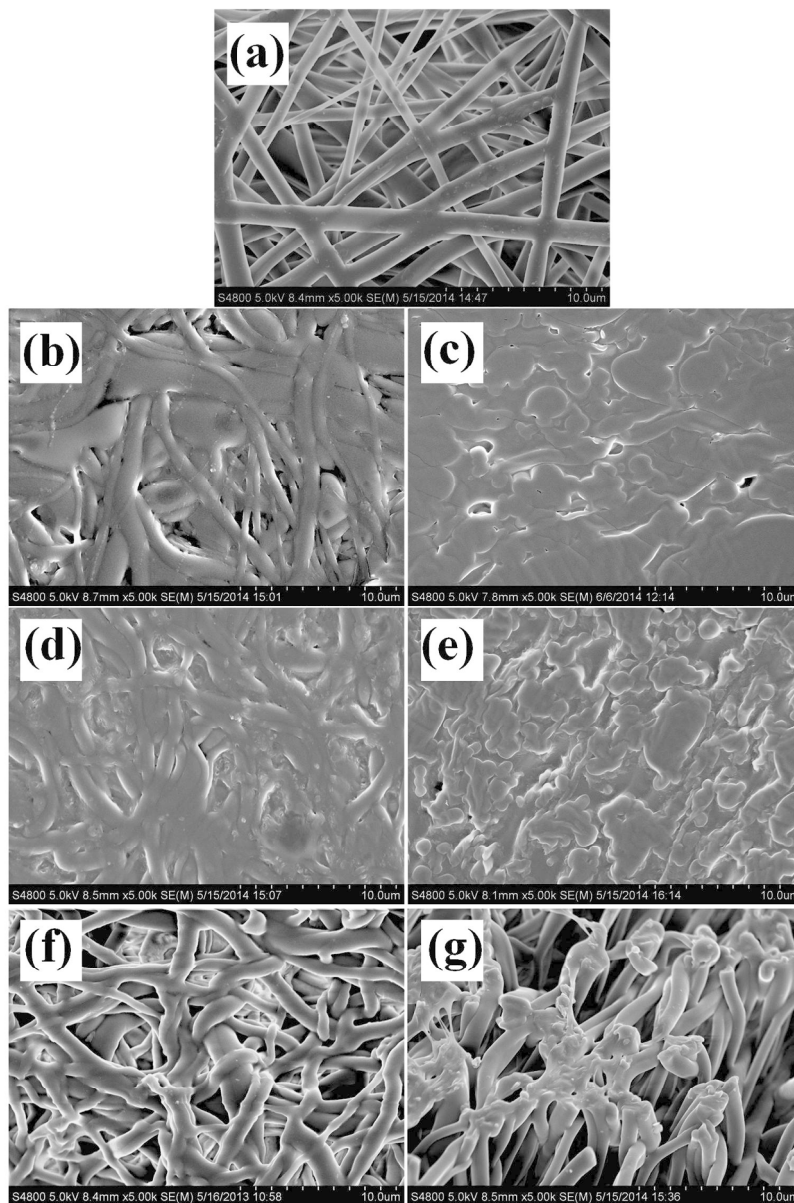297x210mm (150 x 150 DPI)

Figure 3. (a)SEM image of electrospun TPU fibers; SEM images of (b) surface morphology and (c) cross-section morphology of the GG/TPU composite at the mass ratio of 0.25:1; SEM images of (d) surface morphology and (e) cross-section morphology GG/TPU composite at the mass ratio of 0.5:1; SEM images of (f) surface morphology and (g) cross-section morphology the GG/TPU composite films at the mass ratio of 0.5:1 after GG phase was etched
260x385mm (150 x 150 DPI)
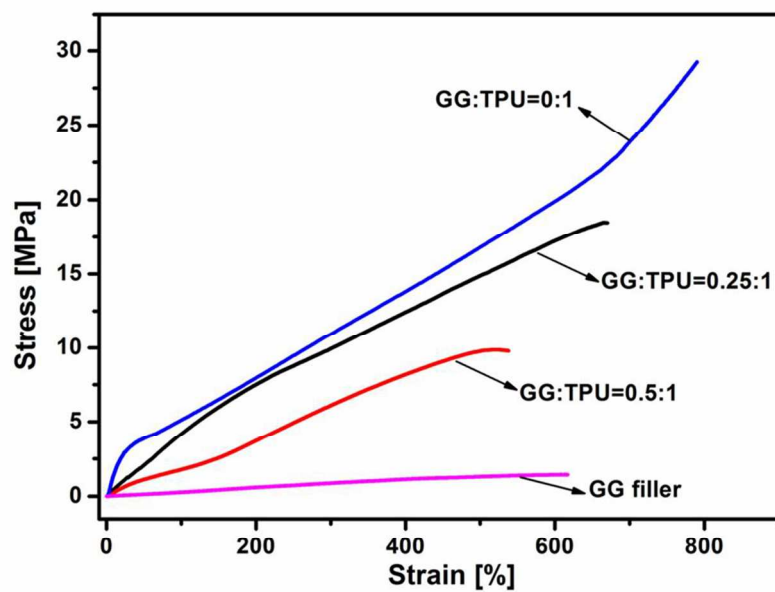
Figure 4. Stress-strain curves of pure TPU, GG/TPU composites, and GG filler
277x196mm (119 x 119 DPI)
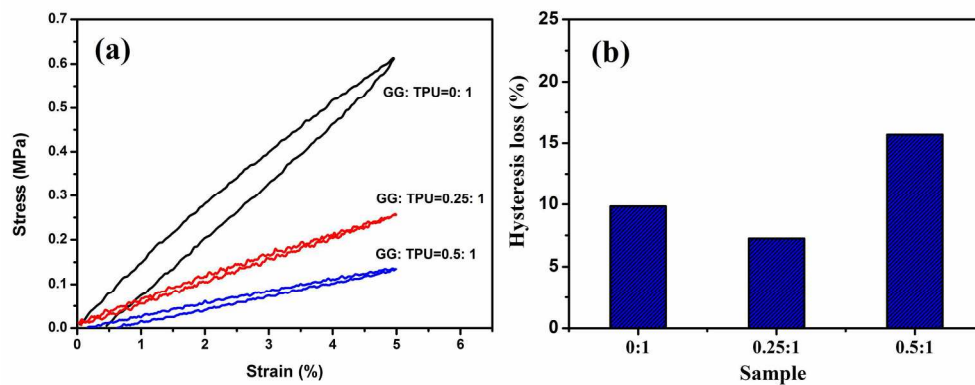
Figure 5. (a)The cyclic stress-strain curves of pure TPU and GG/TPU composites and (b) the corresponding hysteresis loss at 5% of strain
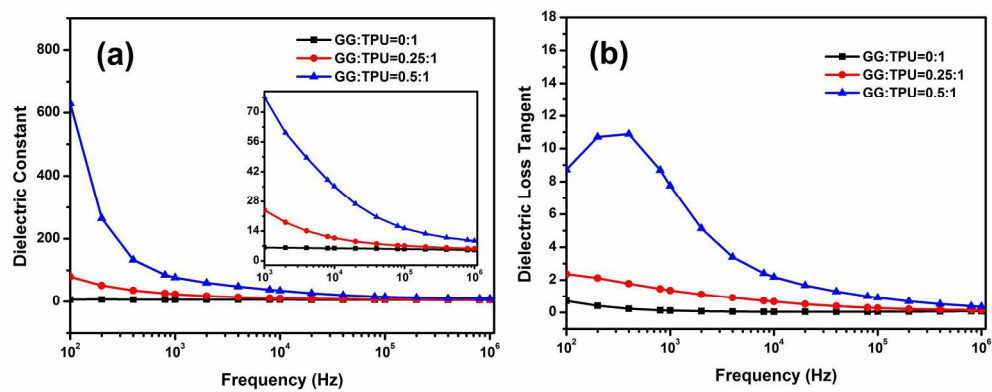427x166mm (150 x 150 DPI)

Figure 6. (a) Dielectric constant and (b) dielectric loss of pure TPU and GG/TPU composites in the frequency range of 10^2 to 10^6 Hz at room temperature
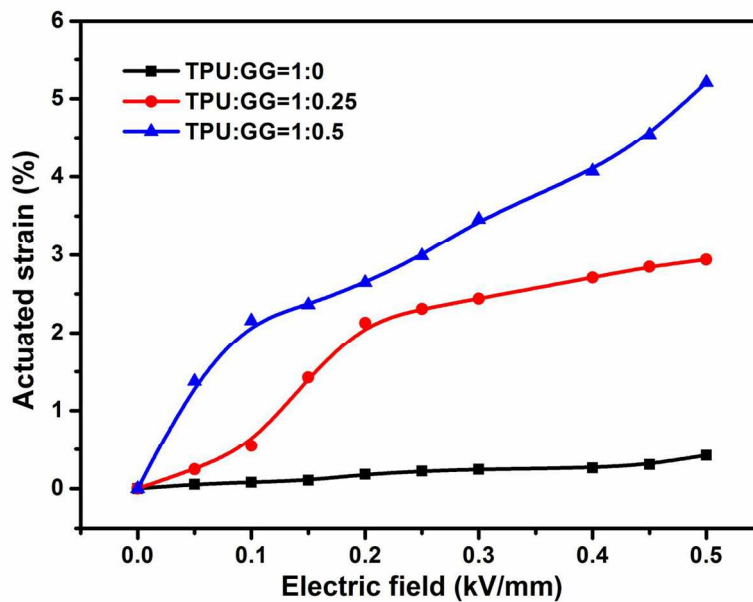417x166mm (150 x 150 DPI)

Figure 7. The actuation strain of TPU and GG/TPU composites at different electric fields
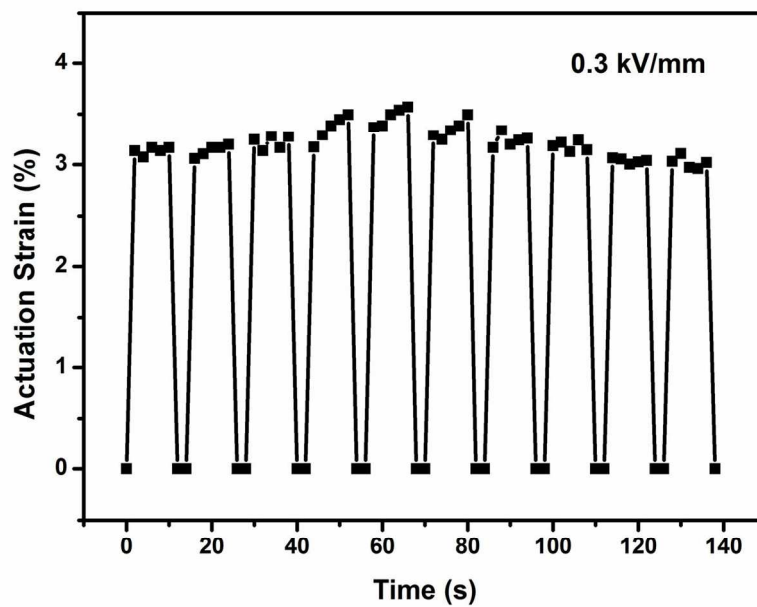297x210mm (150 x 150 DPI)

Figure 8. Plot of actuation strain of GG/TPU composite at the mass ratio of 0.5:1 against cyclic electric field loading
297x210mm (150 x 150 DPI)

Separated-structured all-organic dielectric elastomer with large actuation strain under ultralow-voltage and high mechanical strength

Ming Tian[1, 2] [*], Yang Yao [1], Suting Liu [1, 2], Dan Yang [1, 2], Liqun Zhang[1, 2],

Toshio Nishi[3], and Nanying Ning[1, 2] [*]

1. State Key Laboratory of Organic-Inorganic Composites, Beijing University of Chemical Technology, Beijing 100029, China;
2. Key Laboratory of Carbon Fiber and Functional Polymers, Ministry of Education, Beijing University of Chemical Technology, Beijing 100029, China;
3. Department of Applied Physics, The University of Tokyo, Hongo, Bunkyo-ku, Tokyo, Japan.
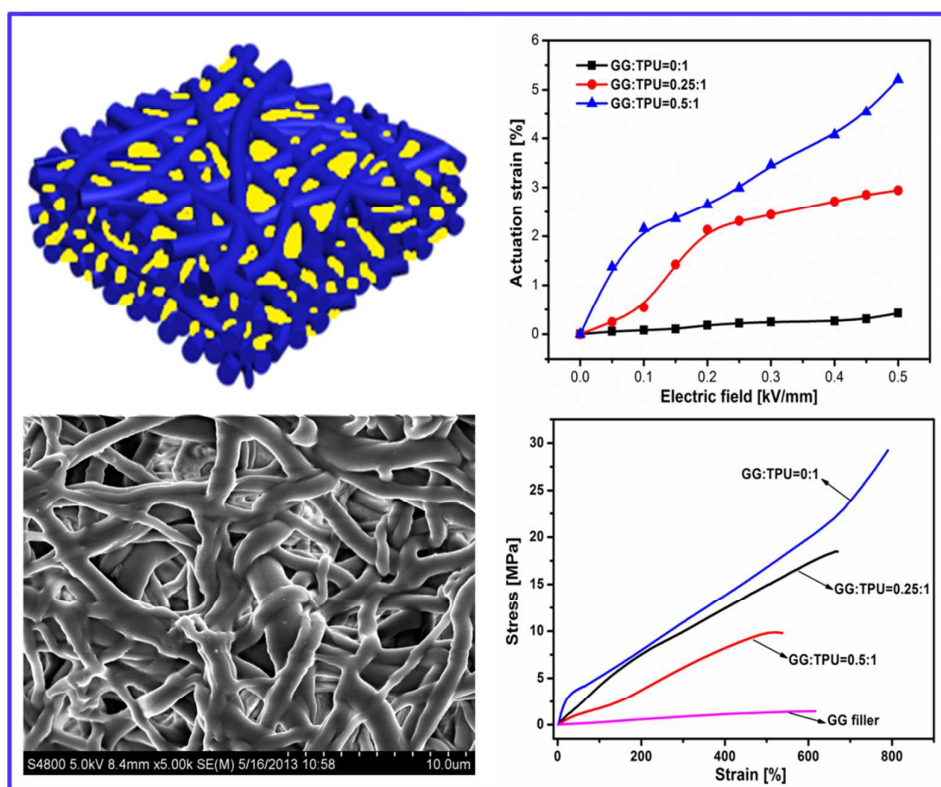
We prepared separated-structured all-organic dielectric elastomer with large actuation strain under ultralow-voltage and high mechanical strength.

[*]**Corresponding author.** College of Materials Science and Engineering, Beijing University of Chemical Technology, No. 15 Bei-San-Huan East Road, ChaoYang District, Beijing, 100029, China. Email:tianm@mail.buct.edu.cn (M. Tian), ningny@mail.buct.edu.cn (N. Ning).